

PAPER • OPEN ACCESS

The effect of in-situ polymerization on PEDOT-PSS/PAN composite conductive fiber

To cite this article: Hu Liu *et al* 2019 *IOP Conf. Ser.: Earth Environ. Sci.* **218** 012161

View the [article online](#) for updates and enhancements.



IOP | ebooks™

Bringing you innovative digital publishing with leading voices to create your essential collection of books in STEM research.

Start exploring the [collection](#) - download the first chapter of every title for free.

The effect of in-situ polymerization on PEDOT-PSS/PAN composite conductive fiber

Hu Liu¹, Yan Gong^{1,*}, Xin Li^{1,*}, Xiuqin Zhang¹, Chongqing Hu¹, Lejun Wang², Yali Pang¹, Cien Fang¹

¹Beijing Key Laboratory of Clothing Materials R&D and Assessment, Beijing Engineering Research Center of Textile Nanofiber, School of Materials Science and Engineering, Beijing Institute of Fashion Technology, Beijing 100029, P. R. China

²Heng Tian Fiber Group Co. Ltd., Beijing 100020, P. R. China

*Corresponding author's e-mail: clylx@bift.edu.cn

Abstract. The in-situ polymerization method was used to prepare poly (3,4- ethylenedioxythiophene dioxide thiophene)-polystyrene sulfonate/polyacrylonitrile (PEDOT-PSS/PAN) composite conductive fiber. The results indicate that more PEDOT particles grow on the surface of in-situ PEDOT-PSS/PAN composite fibers than PAN fiber, which has the conductivity of 9.83 S/cm nearly twice of that of the composite fiber before in-situ polymerization. The crystallinity of the in-situ PEDOT-PSS/PAN composite fiber is a little lower than that of the fiber before in-situ polymerization, but the thermal stability goes by contraries. Furthermore, the in-situ polymerization process has minor effects on the mechanical properties of the fibers. The breaking strengths, elongation at break and initial modulus of the in-situ PEDOT-PSS/PAN composite fiber are 0.67 CN/dtex, 33.90% and 4.63 CN/dtex respectively, which can be waved. It is estimated that this in-situ PEDOT-PSS/PAN composite conductive fiber will have the electromagnetic wave absorption function, which can be used in military as wave absorption material.

1. Introduction

Conductive textile based on conducting polymer combines not only the conduction, electromagnetic shielding and antistatic effect of the traditional conductive textile but also the specific smart sensing feature of conducting polymer^[1-2], such as electrochromism^[3-4], electroluminescence^[5], wettability switching^[6] etc., therefore, it presents great potential for application in fields of novel display device, information storage device, sensor, drug delivery, micro-fluidic device, military camouflage and so on^[7-8]. Among the conducting polymers, poly(3,4-ethylenedioxy-thiophene)-polystyrene sulfonic acid (PEDOT-PSS) has been paid highly attention for its excellent conductive property, high stability and good processability, which usually is solution product, and can be processed by spin coating, silk-screen printing and ink-jet printing etc.^[9-11], therefore, it has attracted much attention and is widely used in electrochromism, electroluminescence and transparent electrode materials^[12-15]. We have done deep studies on preparation and application of PEDOT-PSS. For example, in our previous study, we have obtain the conductive fiber with good electrical conductivity and mechanical properties through wet spinning by compounding the self-made PEDOT-PSS with polyvinyl alcohol (PVA) and polyacrylonitrile (PAN) respectively. The resulted PEDOT-PSS/PAN composite fiber has a conductivity of 5 S/cm, with breaking strength of 0.36 CN/dtex, elongation at break of 36.73 % and



initial modulus of 3.32 CN/dtex, when the PEDOT-PSS content is 1.83% and draw ratio is 4, which presents a good application performance. However, as the conductive fiber, the conductivity of this kind of composite fiber is still too low, and cannot present the specific functions of PEDOT-PSS, further method is still need to improve its conductivity.

In-situ polymerization is favored by researchers as a method building functional composite materials. At previous, we have prepared PEDOT-PSS/polyester composite conductive textile through in-situ polymerization. The resulted composite conductive textile has a conductivity of 2.67×10^{-2} S/cm, which presents electrochromic property with the color change between dark blue and light grey-blue. Besides, we have also prepared polyaniline/cotton composite conductive textile via in-situ polymerization, which can change color between yellow-green and dark green. Through in-situ polymerization, although these textiles have the electrochromic function initially, their properties especially the conductivity need further improve to acquire the application as electrochromic textile.

In this paper, based on the previous study, by further increased the drawing ratio to 6, we obtain the PEDOT-PSS/PAN composite conductive textile with improved breaking strength of 0.73 CN/dtex, then, in-situ polymerization is used for forming the PEDOT-PSS coating on the surface, which is called in-situ PEDOT-PSS/PAN composite conductive fiber. It is found that the conductivity of this kind of fiber is improved for nearly twice, with the conductivity of 9.83 S/cm, which may cause by the synergistic effects between PEDOT-PSS inside the fiber and that on the surface coating, forming the effective conductive paths. It is estimated that this in-situ PEDOT-PSS/PAN composite conductive fiber will have the electromagnetic wave absorption function, which can be used in military as wave absorption material.

2. Experimental

2.1. Materials

Polyacrylonitrile (PAN) was bought from China Daqing Petroleum Refining and Chemical Company, Daqing, China. PEDOT-PSS/PAN Composite fiber was self-made through our previous work^[16]. 3,4-ethylenedioxythiophene (EDOT, $\geq 99.5\%$) was obtained from Suzhou Industrial Park Chemical Reagents Co., Ltd., Suzhou, China. Poly styrene sulfonate (PSS, chemically pure) was gained from Shanghai Jiachen Chemical Co., Ltd., Shanghai, China. Iron trichloride (FeCl_3 , analytical reagent) was purchased from Shantou Xilong Chemical Co., Ltd., Shantou, China. And sodium persulfate ($\text{Na}_2\text{S}_2\text{O}_8$, analytical reagent) was got from Beijing Chemical Factory., Beijing, China. The water used in the synthesis was distilled water. All the reagents were used without further purification.

2.2. Preparation

Pure PAN fiber and PEDOT-PSS/PAN composite fiber were soaked in distilled water for the night and then dried. After that, both the fiber and EDOT were sunk into PSS water solution for a period of time. Then $\text{Na}_2\text{S}_2\text{O}_8$ was added into the solution with stirring, and then FeCl_3 was dropped into the system with the speed of 5 s/drop. Next, the reaction was kept stirring at room temperature for 24 hours. At last, the fiber was taken out and washed with water for several times to get the final products: in-situ PAN conductive fiber and in-situ PEDOT-PSS/PAN composite conductive fiber.

2.3. Characterization

Scanning electron micrographs (SEM) of the fibers were obtained on a JSM-6360LV scanning electron microscope (Japanese electronics company, Japan). The imaging conditions were 10.0 kV and work distance = 29 mm. The structure of the fibers was analyzed by a Nexus 670 Fourier transform infrared (FTIR, Nicolet company, America) spectroscope. X-ray diffraction (XRD) patterns of fiber samples were recorded with Cu K α radiation ($\lambda = 1.5406 \text{ \AA}$) at 40 kV and 50 mA with a Rigaku wide-angle goniometer, (Japan RIGAKU company, Japan). The data were collected in the range $6^\circ \leq 2\theta \leq 36^\circ$. The thermo stability was observed by a TG6300 instrument (SII company, Japan) operating at a heating rate of 10 °C/min under a nitrogen atmosphere. The temperature range was 20-800 °C. The

mechanical properties of the fibers were measured by a YG004N electronic single-fiber tensile strength tester (Nantong Dahong experimental instrument company, China). The electrical conductivities of the samples were examined by a four-probe conductivity meter (Keithley 6221&2182A, Keithley Instruments Inc., America). The conductivities were calculated by the following formula:

$$\delta = IL / VS \quad (1)$$

where δ is the conductivity (S/cm), I is the constant current through the two outer electrodes, L is the distance of the two inner electrodes, V is the variational potential through the two inner electrodes, and S is the area of the fiber section which is calculated by diameters of the fibers obtained via SEM.

3. Results and discussion

3.1. Morphology of the Fibers

Figure 1 shows the morphology of PAN fiber and PEDOT-PSS/PAN composite fiber before and after in-situ polymerization. It is shown that the fiber diameter of the in-situ PEDOT-PSS/PAN composite fiber is about 40 μm , which is larger than that of 25 μm before the in-situ polymerization. Besides, it is clear that the surfaces of both PAN fiber and composite fiber before in-situ polymerization are smooth, but after in-situ polymerization, the fiber surfaces are attached with a lot of particles which are supposed of PEDOT gained from in-situ polymerization. In addition, there are more PEDOT particles on the surface of the in-situ PEDOT-PSS/PAN composite fiber than that of in-situ PAN fiber^[17]. The main reason is: for PEDOT-PSS/PAN composite fibers, there contained PEDOT and EDOT components in the fibers, which have interaction with EDOT monomer in the solution during in-situ polymerization, so the EDOT monomer is easier to diffuse into the composite fiber.

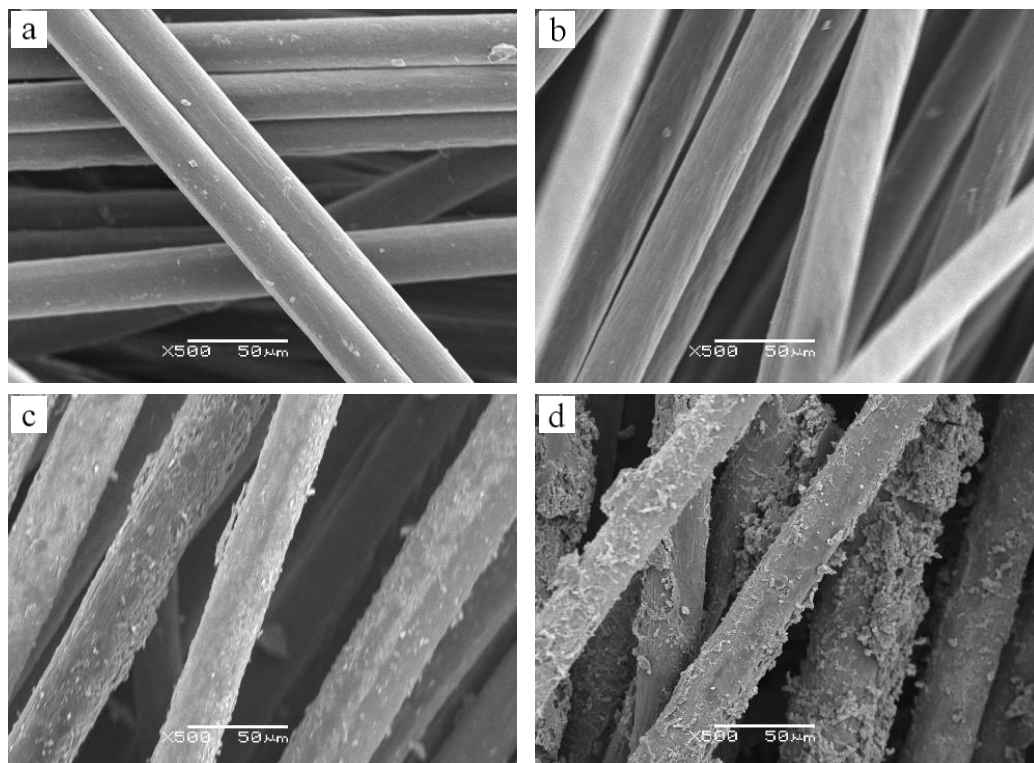


Figure 1. SEM images of the fibers: PAN fiber (a) and composite fiber (b) before the in-situ polymerization; and PAN fiber (c) and composite fiber (d) after the in-situ polymerization

3.2. FTIR spectra of the fibers

The structure of the pure PAN fiber and PEDOT-PSS/PAN composite fiber before and after the in-situ polymerization were measured by FTIR as shown in Figure 2. In the absorption curves of Figure 2a and 2b, the strong and broad peaks at 3426 cm^{-1} are assigned as hydrostatic bond stretching vibration peaks, and the sharp peaks at 2062 cm^{-1} are associated to those stretching vibrations of $-\text{SCN}$ of sodium thiocyanate generated during the wet-spinning process. Besides, the absorption peak at 2935 cm^{-1} is methylene anti-symmetric stretching vibration and the absorbance at 1724 cm^{-1} belongs to $-\text{C}=\text{O}$ of those ester compounds added into PAN powder originally to promote dyeing, and the peaks at 2249 cm^{-1} result from the stretching vibration of $-\text{C}\equiv\text{N}$ as well^[18]. In Figure 2b, the absorption peaks at 1532 cm^{-1} and 1630 cm^{-1} are the stretching vibration peaks of the benzene ring in the PSS^[19-20], and the peak around 980 cm^{-1} is attributed to the stretching vibration peak of $-\text{C}-\text{S}-\text{C}-$ of EDOT. Figure 2c and 2d are similar with each other, and the peaks of them are all weaker than that of Figure 2a and 2b, in addition, some peaks have disappeared such as the peaks at 3426 cm^{-1} and 2062 cm^{-1} , the former demonstrating there is no hydrostatic bond anymore after in-situ polymerization, and the later indicating that there no sodium thiocyanate on the surface of fibers after in-situ polymerization. At the same time, the characteristic peaks of PEDOT/PSS at 1532 cm^{-1} and 1630 cm^{-1} which are belongs with benzene ring of PSS and the absorption of $-\text{C}-\text{S}-\text{C}-$ at 980 cm^{-1} still exist, which indicates the forming of PEDOT on the surface of the fibers.

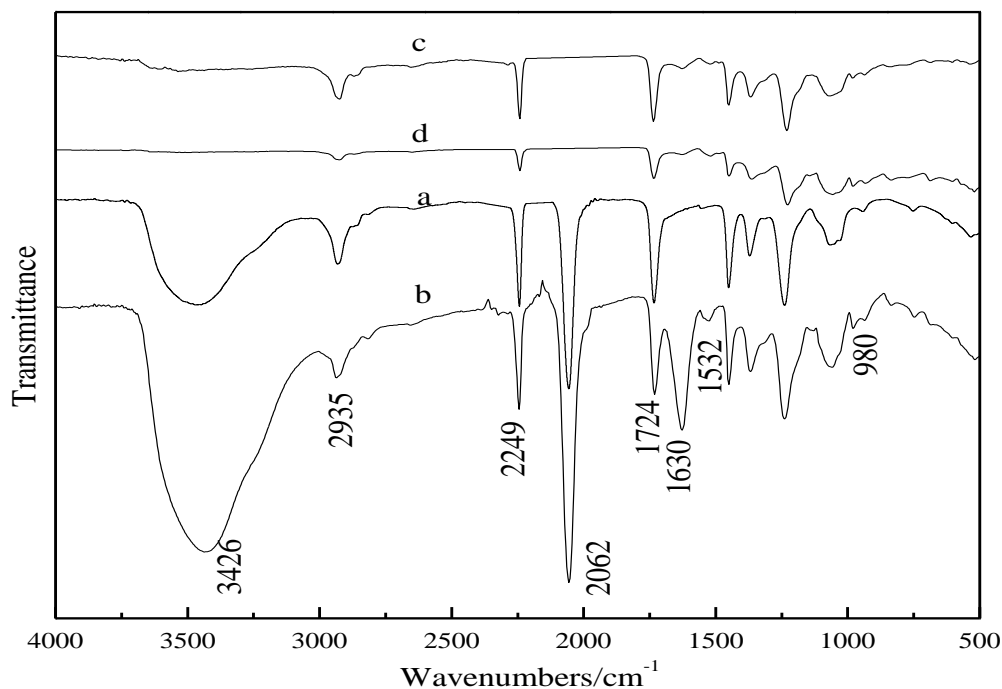


Figure 2. FTIR of the fibers: PAN fiber (a) and composite fiber (b) before the in-situ polymerization; and PAN fiber (c) and composite fiber (d) after the in-situ polymerization

3.3. XRD spectra of the fibers

The XRD patterns of PAN fiber and composite fiber before and after in-situ polymerization are shown in Figure 3. Differences between both PAN fiber and PEDOT-PSS/PAN composite conductive fiber before and after polymerization exist in XRD curves although they are similar with each other. Obviously, for all XRD patterns in Figure 3, the strongest diffraction peak occurs at around $2\theta=17^\circ$, which can be indexed to the (100) plane of a hexagonal structure of PAN^[21]. The broad diffraction peaks centered at 27° indicate that the crystallization of all the fibers is amorphous phase. Compare the four curves, it can be seen that both the peak value at 17° and 27° decrease in turn of : a > b > c > d. The

smallest peak value indicates the strongest amorphous state, which comes from a great quantity of amorphous PEDOT on the surface of the fiber increasing the area of the amorphous region.

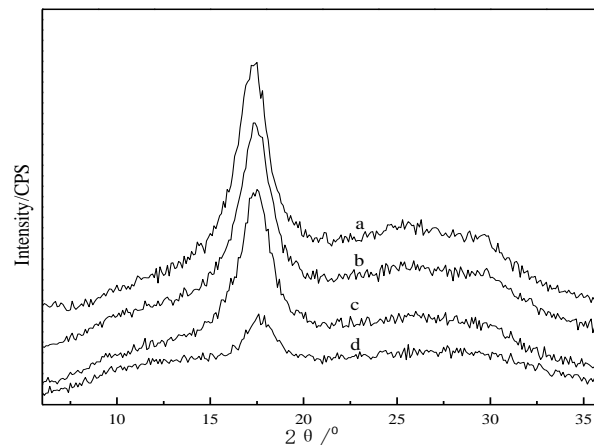


Figure 3. XRD patterns of the fibers: PAN fiber (a) and composite fiber (b) before the in-situ polymerization; and PAN fiber (c) and composite fiber (d) after the in-situ polymerization

3.4. TG curves of the fibers

Thermal stability of the four fibers is studied by TG, which is an important method to detect the degradation behavior of the fibers. From Figure 4, it is clear that the TG curves of PAN fiber and composite fiber before the in-situ polymerization are similar with each other and the two fibers after in-situ polymerization are similar, respectively. For the two fibers before in-situ polymerization, the first weight loss of 4~9 wt% at 100 °C is attributed to the elimination of moisture absorbed^[22], and the second one at 280~550 °C^[23] represents the degradation of the PAN molecular chains, and the final amount of residual carbon is from 62 to 64%. For the two fibers after in-situ polymerization, the first weight losses of 1~2 wt% occur at 70 °C and the second one at 310~580 °C with the residual carbon of 36-43%. Comparing these two kinds of fibers of before and after in-situ polymerization, we know that the initial decomposition temperature, the first weight losses amount and the residual carbon of the former fibers are all higher than that of the latter, but the second weight loss temperature of the former is lower than that of the latter. The higher residual carbon of the fibers before in-situ polymerization may due to the inorganic impurity from the wet spinning. In summary, from Figure 5, it indicates that the thermal stability of fibers after in-situ polymerization is slightly better than that of the fibers before in-situ polymerization.

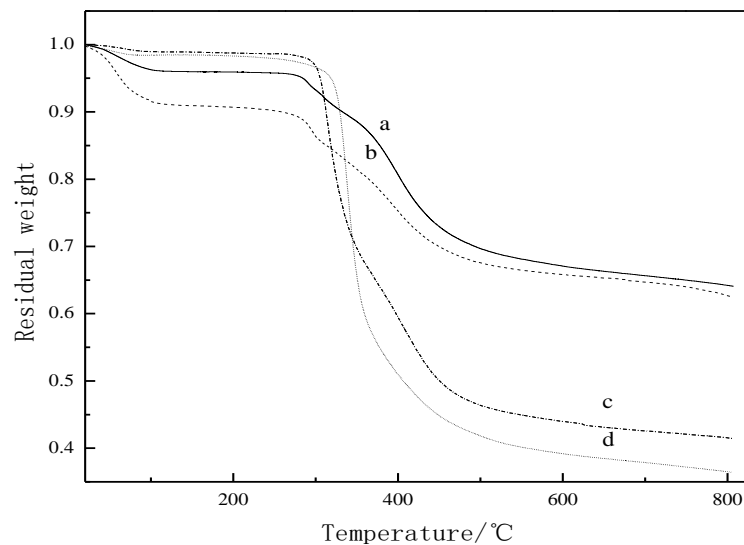


Figure 4. TG curves of the fibers: PAN fiber (a) and composite fiber (b) before the in-situ polymerization; and PAN fiber (c) and composite fiber (d) after the in-situ polymerization

3.5. Conductivity of the fibers

It is known that the pure PAN fiber is non-conductive, but after in-situ polymerization, as shown in Table 1, the conductivity of PAN fiber increased to 0.024 S/cm. The conductivity of the composite fiber is 4.98 S/cm, while the conductivity of the in-situ PEDOT-PSS/PAN composite fiber is 9.83 S/cm, which is nearly twice of the former. During the in-situ polymerization, the PEDOT-PSS/PAN composite fiber are soaked in the solution containing EDOT, as the synergetic action between EDOT in the solution and PEDOT in the composite fiber, more PEDOT grow on the surface of PEDOT-PSS/PAN composite fiber. As a result, the in-situ PEDOT-PSS/PAN composite fiber has much higher PEDOT content and conducting path than that of pure PAN fiber after in-situ polymerization, and of course having higher conductivity.

Table 1. The conductivity of PAN fiber after in-situ polymerization and composite fiber before and after in-situ polymerization

Fibers	Conductivity (S/cm)
PAN fiber after in-situ polymerization	0.024
Composite fiber before in-situ polymerization	4.98
Composite fiber after in-situ polymerization	9.83

3.6. Mechanical property of the fibers

Table 2 gives the mechanical properties of the four fibers. It can be seen that the breaking strength of PAN fibers before and after polymerization is 0.79 CN/dtex and 0.73 CN/dtex respectively, while that of composite fibers is 0.72 CN/dtex and 0.67 CN/dtex respectively, which indicates that the in-situ polymerization process has little effect on fiber strength. But observing the dates of both the elongation at break and initial modulus, it is found that they are decreased compared with that of PAN fibers before and after in-situ polymerization. Therefore, in-situ polymerization process have a certain reduce on the mechanical properties of PAN fiber, however it does not affect their application for mechanical woven.

Table 2. Mechanical properties of PAN fiber and composite fiber before and after in-situ polymerization

Fibers	Breaking strengths (CN/dtex)	Elongation at break (/%)	Initial modulus (CN/dtex)
PAN fiber before in-situ polymerization	0.79	49.91	5.06
PAN fiber after in-situ polymerization	0.72	50.23	5.38
Composite fiber before in-situ polymerization	0.73	33.23	3.97
Composite fiber after in-situ polymerization	0.67	33.90	4.63

4. Conclusions

This paper studies the effect of in-situ polymerization on the PAN fiber and PEDOT-PSS/PAN composite fiber, and draws the following conclusions:

1. After the in-situ polymerization, the crystallinity of both PAN fiber and composite fiber have a certain decreased.
2. The thermal stability of fibers after in-situ polymerization is slightly better than that of the fibers before in-situ polymerization.
3. The conductivity of the in-situ PEDOT-PSS/PAN composite fiber has increased to about 2 times compared with that of composite fiber before in-situ polymerization.
4. The mechanical property of in-situ PEDOT-PSS/PAN composite fiber is a certain reduced compared with pure PAN, but does not affect its application for mechanical woven.
5. This kind of in-situ PEDOT-PSS/PAN composite fiber is expected to be used in electromagnetic wave absorption field.

Acknowledgements

This project was financially supported by the National Nature Sciences Foundation of China (51873003, 21544002), Special funds for the construction of high level teachers of Beijing Institute of Fashion Technology (BIFTXZ201802, BIFTTD201801), Open Project Program of 17312 Beijing Key Laboratory of Ergonomics and Functional Innovation Design (KYTG02170202) and Beijing Great Wall Scholars Incubator Program (CTT&TCD20180321).

References

- [1] Zhou J., Mulle M., Zhang Y., Xu X., Li E., Han F., Thoroddsen S. T., Lubineau G. (2016) High-ampacity conductive polymer microfibers as fast response wearable heaters and electromechanical actuators. *J. Mater. Chem. C.*, 4: 1238-1249.
- [2] Meng J., Li X., Qin M., Pei Y., Yang S., Lan Y., Wang R., Chen G. (2017) Effects of pore size of reverse opal structured PEDOT films on their electrochromic performances. *Org. Electron.*, 50:16-24.
- [3] Dirk S., Michael V., Volker B., Erik F., Michael R. B. (2014) Flexible, Switchable Electrochromic Textiles. 3: 330-335
- [4] Fern, M. K., Ludivine, M., Cedric, C., Vladan, K. (2013) Evaluation of Solid or Liquid Phase Conducting Polymers Within a Flexible Textile Electrochromic Device. *J. Disp. Technol.*, 9:626-631.
- [5] Hu B., Li D., Okan A., Prakash M. (2011) Textile - Based Flexible Electroluminescent Devices. 2:305-311.
- [6] Jin P., Zhang D., Li X., Zhao L. (2010) Doping/dedoping Process in Duced Wettability Switch of Polyaniline-coated Conductive Textile. *Act. Poly. Sin.*, 2:192-198.
- [7] Nuramdhani I., Gokceoren A. T., Odhiambo S. A., De M. G., Hertleer C., Van L. L. (2018)

- Electrochemical Impedance Analysis of a PEDOT:PSS-Based Textile Energy Storage Device. *Mater.*, 11:1-11.
- [8] Ken-ichi N., Yoshinori H., Shusuke K., Yasuyuki K., Hirobumi, U. (2018) Fabrication of a Textile-Based Wearable Blood Leakage Sensor Using Screen-Offset Printing. *Sensors.*, 18:1-11
- [9] Yu Z., Li C., Abbitta D., Thomas J. (2014) Flexible, sandwich-like Ag-nanowire/PEDOT:PSS-nanopillar/MnO₂ high performance supercapacitors. *J. Mater. Chem. A.*, 2:10923-10929.
- [10] Zhou J., D. H. Anjum, Chen L., Xu X., Ventura I. A., Jiang L., Lubineau G. (2014) The temperature-dependent microstructure of PEDOT/PSS films: insights from morphological, mechanical and electrical analyses. *J. Mater. Chem. C.*, 2:9903-9910.
- [11] Suchol S., Esther C., Sandro M. R., Adam D. P., Aliaksandr V. Z., Timothy F.O.C., Daniel R., Eduardo V., Darren J. L. (2015) Effect of Broken Conjugation on the Stretchability of Semiconducting Polymers. *Adv. Funct. Mater.*, 25:427-436.
- [12] Haizeng L., Liam M., Abdulhakem Y. E. (2018) Solution-Processed Interfacial PEDOT:PSS Assembly into Porous Tungsten Molybdenum Oxide Nanocomposite Films for Electrochromic Applications. *ACS. Appl. Mater. Inter.*, 10:10520-10527.
- [13] 1. Anderson E. X. G., Gustavo H. S., Edgar H. de S., Paula C. R., João B. F., Ricardo C. K., Jeferson F. de D., Andreia G. M. (2017) Influence of electrolyte distribution in PEDOT:PSS based flexible electrochromic devices. *Chem. Phys. Lett.*, 689:212-218.
- [14] Li X., Zheng Y., Zhang Y., Li C., Chen G. (2017) PEDOT-PSS/PVA Composite Conductive Textile with Electromagnetic Wave Absorption Properties Prepared by in situ Polymerization. *Acta. Polym. Sin.*, 4:661-668.
- [15] Wan C., Jiana C., Cho E.C., Yen S., Ho B., Lee K., Huang J., Hsiao Y. (2018) Facile preparation of WO₃/PEDOT:PSS composite for inkjet printed electrochromic window and its performance for heat shielding. *Dyes. Pigments.*, 148: 465-473.
- [16] Liu Y., Li X., Li C. (2013) Electrically conductive poly(3,4 - ethylenedioxythiophene)–polystyrene sulfonic acid/polyacrylonitrile composite fibers prepared by wet spinning. *J. Appl. Polym.*, 130:370-374.
- [17] Li X., Liu Y., Shi, Z., Li C., Chen G. (2014) Influence of draw ratio on the structure and properties of PEDOT-PSS/PAN composite conductive fibers. *Rsc. Adv.*, 4:40385-40389.
- [18] Malaisamy S., Priyanka P., Paramasivam M. (2014) Development of quasi-solid-state dye-sensitized solar cell based on an electrospun polyvinylidene fluoride–polyacrylonitrile membrane electrolyte. *J. Appl. Polym. Sci.* 131: 41107(1-8).
- [19] Kun Z., Shiren W. (2015) Fabrication of Two-Dimensional PEDOT:PSS Nanosheets Through In Situ Formed Complexes. *Nano.*, 10:15500(1-5).
- [20] Shan X., Zhang L. Y., Lu X., (2013) Conductivities enhancement of poly(3,4-ethylenedioxythiophene)/poly(styrene sulfonate) transparent electrodes with diol additives. *Polym. Bull.*, 70:237-247.
- [21] Xia Y., Lu Y. (2010) Conductive polymers/polyacrylonitrile composite fibers: Fabrication and properties. *Polym. Compos.*, 31:340-346.
- [22] Takahashi T., Ishihara M., Okuzaki. (2005) Poly(3,4-ethylenedioxythiophene)/poly(4-styrenesulfonate) microfibers. *H. Synth. Met.*, 152: 73-76.
- [23] Toptaş N., Karakışla M., Saçak M. (2009) Conductive polyaniline/polyacrylonitrile composite fibers: Effect of synthesis parameters on polyaniline content and electrical surface resistivity. *Polym. Compos.* 30:1618-1624.